Microfluidics-Assisted Assembly of Injectable Photonic Hydrogels toward Reflective Cooling

Zhijie Zhu,Ji-Dong Liu,Chang Liu,Xingjiang Wu,Qing Li,Su Chen,Xin Zhao*,David A. Weitz

Abstract

Development of fast curing and easy modeling of colloidal photonic crystals is highly desirable for various applications. Here, a novel type of injectable photonic hydrogel (IPH) is proposed to achieve self-healable structural color by integrating microfluidics-derived photonic supraballs with supramolecular hydrogels. The supramolecular hydrogel is engineered via incorporating β-cyclodextrin/poly(2-hydroxypropyl acrylate-co-N-vinylimidazole) (CD/poly(HPA-co-VI)) with methacrylated gelatin (GelMA), and serves as a scaffold for colloidal crystal arrays. The photonic supraballs derived from the microfluidics techniques, exhibit excellent compatibility with the hydrogel scaffolds, leading to enhanced assembly efficiency. By virtue of hydrogen bonds and host–guest interactions, a series of self-healable photonic hydrogels (linear, planar, and spiral assemblies) can be facilely assembled. It is demonstrated that the spherical symmetry of the photonic supraballs endows them with identical optical responses independent of viewing angles. In addition, by taking the advantage of angle independent spectrum characteristics, the IPH presents beneficial effects in reflective cooling, which can achieve up to 17.4 °C in passive solar reflective cooling. The strategy represents an easy-to-perform platform for the construction of IPH, providing novel insights into macroscopic self-assembly toward thermal management applications.

1 Introduction

Recently, colloidal photonic crystals (CPCs) have drawn tremendous attention due to their potentials in chemical sensors,1 optical display,2 energy conversion,3 and others. In particular, their bright structural colors derived from photonic bandgap (PBG) are highly associated with self-assembly efficiency of colloidal particles.4 To this end, great efforts are devoted to enhancing self-assembly efficiencies of CPCs, such as ink-jet printing,5 Langmuir–Blodgett method6 and microfluidics.7 Among them, the microfluidics technique has emerged as a powerful tool to achieve facile construction of this structure due to its controllability and processability. In this respect, Gu's group investigated droplet microfluids for the construction of colloidal crystal fibers or beads with either anisotropic angle independence or full angle independence.8 Aizenberg and co-workers demonstrated that the multiple optical effect of spherical colloidal crystals was attributed to their complex microstructures.9 By applying the microfluidics-assisted self-assembly method, our group have constructed responsible photonic supraballs as well as Janus particles with controllable and predictable shape.10 Unfortunately, fast curing and easy modeling of CPCs with desired morphology is still challenging as the conventional assembly process highly relies on the time-consuming evaporation-mediated colloidal rearrangement. For instance, most energy involved applications, such as photocatalysis, supercapacitors and reflective cooling by CPCs suffer from low assembly efficiency, thereby limiting their scaled-up production.11 This motivates us to develop new strategies for facile and fast construction of CPCs toward energy applications.

Here, we developed an available easy-to-perform strategy for facilely curing CPCs with structural colors in a large-scale and fast fashion. Inspired by the reported supramolecular hydrogels for additive manufacturing,12 we mixed microfluidics-derived CPC supraballs (structural coloration material) with self-healable hydrogel (scaffold) as the assembly unit, producing a new kind of injectable photonic hydrogel (IPH) in situ. The IPH had both self-healable and temperature-controllable abilities. We initially synthesized monodisperse polystyrene@poly(2-hydroxypropyl acrylate-co-N-vinylimidazole) (PS@poly(HPA-co-VI)) core/shell colloidal microspheres (Figure 1a). Such microspheres with high amount of carboxyl and imidazole groups could serve as assembly units for the construction of photonic supraballs via a microfluidics technique (Figure 1b). Then, a supramolecular system comprising β-cyclodextrin (host) and N-vinylimidazole (guest) was introduced into methacrylated gelatin (GelMA), allowing the formation of covalently crosslinked network with enhanced mechanical strength. By taking advantage of the phase transition of the supramolecular hydrogel precursor upon temperature stimuli, IPH solution was transformed into a solid hydrogel outside the syringe, resulting in a physically crosslinked photonic hydrogel (Figure 1c). After photopolymerization, the photonic hydrogels with a fixed structure could be achieved. Accordingly, a series of linear, planar and spiral assemblies with refined micro- and nanoscale structure, uniform morphologies and enriched colors could be realized via a microfluidics-assisted assembly strategy. In addition, such photonic gel was utilized as a reflective cooler with a fascinating temperature management effect. This work has the following attractive advantages: 1) using temperature-dependent phase transition of IPH to facilely cure CPC supraballs in a controllable and fast fashion; 2) developing the IPH for fast modeling CPCs into various ordered structures, such as linear, planar, and spiral photonic crystal assemblies; 3) exploring new applications of IPH in reflective cooler by the effect of angle-independent selective reflection. We therefore believe that our strategy represents a facile and easy-to-perform pathway for the construction of versatile IPH, which may pave the way for further applications of structural colored materials.

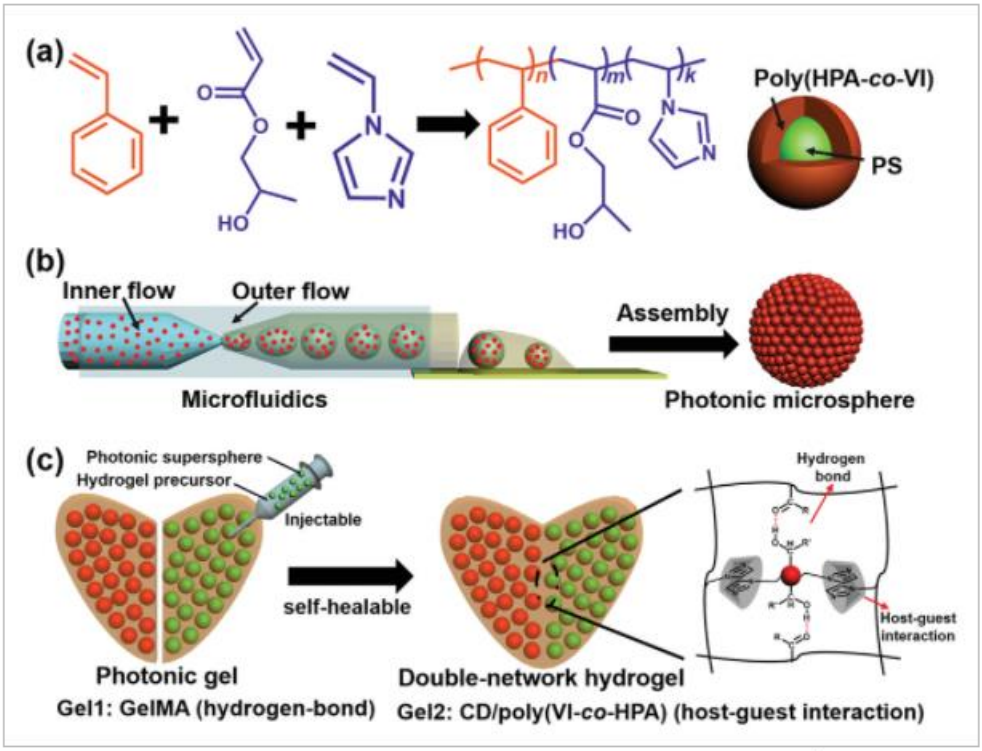

Figure 1 Open in figure viewer | PowerPoint

a) Synthesis routes for monodisperse PS@poly(HPA-*co*-VI) core/shell colloidal microspheres via seed emulsion polymerization. b) Schematic of emulsion-droplet preparation of dispersions via microfluidics. The resulting droplets are then dried in air. c) Cartoon illustration of preparation of photonic hydrogel using an injectable hydrogel system composed of hydrogel scaffold and photonic supraballs.

2 Results and Discussion

2.1 Microfluidics-Directed Assembly of Core/Shell Colloidal Microspheres

The microfluidics assembly process (with colloidal microspheres as the building blocks) started from the synthesis of monodisperse core/shell colloidal microspheres by seed emulsion polymerization.13 The microspheres abbreviated as PS@poly(HPA-co-VI) are composed of a polystyrene (PS) core and a copolymer shell prepared by 2-hydroxypropyl acrylate and N-vinylimidazole. The transmission electron microscope (TEM) image of PS@poly(HPA-co-VI) microspheres revealed that the particles were spherical in shape, and possess a well-defined core/shell architecture (Figure S1, Supporting Information). We further carried out Fourier-transform infrared (FT-IR) measurements of the product to analyze the chemical composition of PS and PS@poly(HPA-co-VI) microspheres. Along with the introduction of poly(HPA-co-VI) shell, a new characteristic absorption peak at 1289 cm−1 could be observed, which is attributed to the ring vibration of imidazole groups (Figure S2, Supporting Information).14 Therefore, we argue that the synthesis of core/shell PS@poly(HPA-co-VI) colloidal microspheres was successful and the microspheres possessed a high amount of hydroxyl and imidazole groups. This character makes the PS@poly(HPA-co-VI) colloidal microspheres a good candidate to form IPH by hydrogen bonds and host–guest interactions.

To form CPC supraballs, we used a single-emulsion capillary microfluidics device to generate water-in-oil emulsion droplets.15 The inner discontinuous phase (PS@poly(HPA-co-VI) emulsion)

was broken into microdroplets at the tip of the dripping regime of the inner capillary tube by an outer continuous phase (methylsilicone oil). After water was completely evaporated, the PS@poly(HPA-co-VI) microspheres were closely packed into a highly ordered colloidal crystal structure. Generally, the supraball size is essential to the microfluidics-assisted assembly and it has a close relationship with the inner and outer flow rate as well as colloidal concentration. The 3D surface map and the corresponding contour map that represent the relationship between microfluidics parameters (inner flow rate/outer flow rate, colloidal latex concentration) and particle size are shown in Figure 2a,b. The emulsification exhibited good stability and feasibility with inner flow rate, outer flow rate and colloidal concentration fixed at 0.1, 10 mL h−1, and 0.2 g mL−1, respectively. Therefore, a series of CPC supraballs with different reflections could be achieved by varying the diameters of PS@poly(HPA-co-VI) microspheres (Figure 2c). Four photonic supraballs with blue (439 nm), green (514 nm), yellow (565 nm), and red (618 nm) structural colors were prepared from PS@poly(HPA-co-VI) microspheres with diameters of 185, 216, 238, and 260 nm, respectively. In particular, a linear correlation between the diameter of PS@poly(HPA-co-VI) microspheres and photonic stopband was noted (Figure S3, Supporting Information), which is in good agreement with the Bragg's law. These supraballs were highly uniform with diameters of ≈300 μm. The microstructure of the colloidal supraball was characterized by scanning electron microscopy (SEM), as seen in Figure 2d. It is clear that the hard PS@poly(HPA-co-VI) microspheres mostly crystallized into a hexagonal closely packed symmetric structure at the surface of the supraball. Such highly ordered surface is sufficient to promote the Bragg diffraction as evidenced by the reflection spectra (Figure 2e).16 Additionally, the as-prepared photonic supraballs exhibit excellent water stability and no obvious structural changes was detected after stored in water for up to 12 h (Figure S4, Supporting Information). This feature confers the photonic supraballs ideal candidate for the construction of photonic hydrogels. This microfluidic strategy enables the large-scale production of bright colorful CPC supraballs in a controllable and continuous manner.

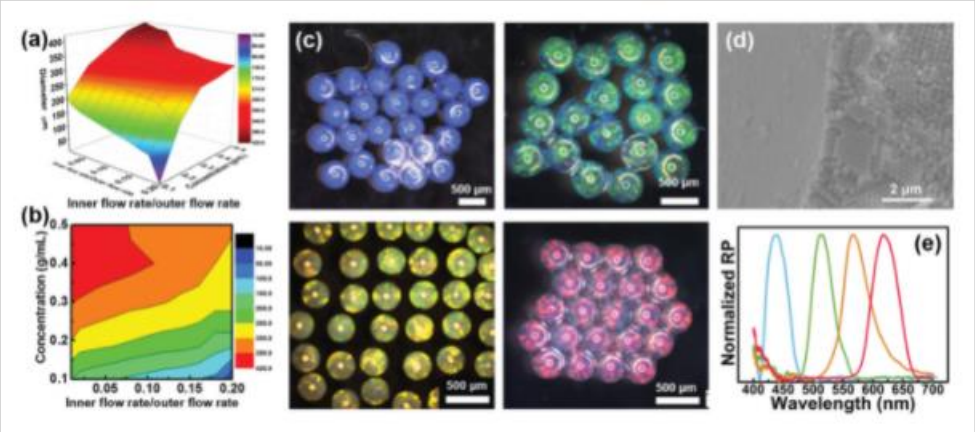

Figure 2

Open in figure viewer | PowerPoint

a,b) The relationship of diameter of photonic supraballs with inner and outer flow rate, and emulsion concentration. c) Optical micrographs of four photonic supraballs fabricated from PS@poly(HPA-*co*-VI) microspheres with different diameters. d) SEM image of the cross-section of a photonic supraballs. e) Reflection spectra of photonic supermicrospheres with different structural colors: blue (439 nm), green (514 nm), yellow (565 nm), and red (618 nm)

2.2 Injectable Photonic Hydrogel Containing Microfluidics-Derived Supraballs

We further investigated the construction of photonic hydrogels by using the microfluidics-derived supraballs as structural coloration materials. Unlike crystallizing monodisperse microspheres into highly ordered colloidal crystals by self-assembly methods, we attempted to disperse photonic supraballs in the hydrogel precursor and used the mixture as building blocks to construct IPH.17 In this respect, GelMA was used as a scaffold to embed the photonic supraballs due to its photocurable ability and temperature-adjustable viscosity.18 To overcome intrinsic poor mechanical property of GelMA, a host–guest supramolecular hydrogel (CD/poly(HPA-co-VI)) was incorporated into GelMA by simply blending them together. Figure 3a,b shows the physical formation of both the binary hydrogel precursor and photonic hydrogel precursor under different temperatures. It is obvious that the viscosity of the binary mixture decreased with the increasing temperature, and the gelation occurred in seconds when the temperature was below ≈20 °C. We conducted the rheological study to analyze the temperature dependent phase transition property of the mixture gel. As expected, the viscosity of the GelMA/CD/poly(HPA-co-VI) hydrogel precursor decreased with increasing temperature (Figure S5, Supporting Information). Subsequently, taking advantage of this temperature-dependent phase transition property, the photonic hydrogel precursor containing the photonic supraballs as structural coloration material and binary hydrogel as scaffold was injected into a mold (Figure 3c). As soon as the photonic hydrogel precursor was extruded into the mold (temperature below 20 °C), gelation occurred and the mixture was transformed into a solid hydrogel. It is worth mentioning that such gelation process was reversible, that is, it could be reproduced by temperature change cycles. Meanwhile, the photonic gel with a fixed structure was obtained by photopolymerization under UV light (365 nm).

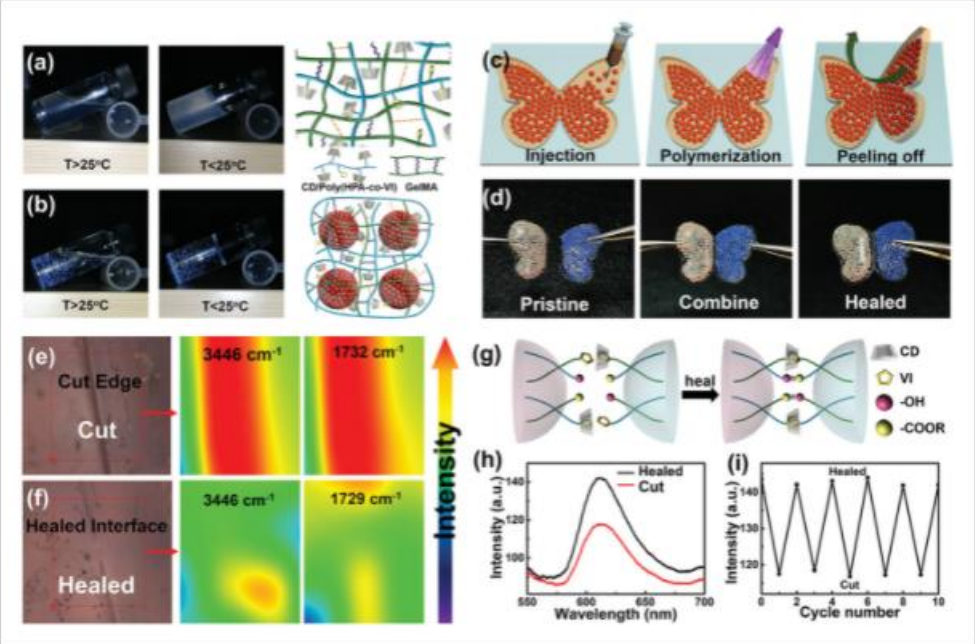

Figure 3

Open in figure viewer | PowerPoint

Sol–gel transition of a) pregel solution and b) supraball/pregel solution upon temperature stimuli. c) Schematic of preparation of photonic hydrogels. The process can be divided into three steps: injection, polymerization and peeling off. d) Self-healing process of the butterfly-shaped photonic hydrogel: two individually prepared photonic hydrogel were combined into one integral photonic hydrogel. e,f) Optical images (left), and IR images (right) of photonic gel. e) Cut edge; f) healed interface. g) Schematic of the self-healing procedure. h) Reflectance spectra of cut area before and after self-healing. i) Variation of reflection intensity under repeated cut-repair treatment.

We further evaluated the self-healing capacity of the photonic gel by a macroscopic test and infrared imaging (IR imaging) characterization. Two halves of butterfly-shaped photonic hydrogels were brought into contact at ambient temperature. After several minutes, the two closely placed pieces rapidly recombined into an intact butterfly-shaped photonic hydrogel without any external stimulus. The joint between the two blocks is strong enough to be lifted (Figure 3d). The mechanical strength of photonic hydrogel after self-healing is close to that of the original sample, revealing good self-healing efficiency (Figure S6, Supporting Information). The IR images that provide definitive evidence for the revolution of oxygen-containing functional groups from the cut area and the healed area are shown in Figure 3e,f. Analogous to the self-healable hydrogels reported previously, the freshly fractured sample contains many active groups on their surface, such as carboxylic groups (≈1730 cm−1) and hydroxyl groups (≈3400 cm−1). Conversely, these oxygen-containing groups became relatively uniform after healing, suggesting that intermolecular hydrogen bonding was responsible for inducing recombination (Figure 3g). Moreover, a red photonic gel was adopted to study the reliability of the self-healing process. The strong reflectance sharply decreased after blade cut while recovered after healing (Figure 3h). We monitored the reflectance after ten times self-healing cycles, and the diffraction intensity returned to its original position, indicating good reversibility and durability (Figure 3i). Comparing with the photonic crystals prepared by direct crystallization, this strategy offers new opportunities by injecting mixture of photonic supraballs and hydrogel precursor into colorant structure.

2.3 Dot-In-Line Photonic Hydrogels by Microfluidics-Assisted Assembly

Another advantage of our IPH is its low angle dependent structural color due to the spherical symmetry. In this case, each constituent photonic supraball could form the same photonic bandgap, resulting in identical reflective color from the photonic hydrogel (Figure 4a).19 To demonstrate such property, we collected the optical images of the butterfly-shaped photonic gel at different viewing angles. The reflecting colors were invariant when the view angle changed from 0° to 75° (Figure 4b). Moreover, Figure 4c gives quantified evidence for the angle-independent optical hydrogel, where the band positions remained unchanged, which is consistent with the above optical images. The conventional angle-independent structural color was often fabricated by virtue of amorphously arranged colloidal particles, which is noniridescent and has a high affinity to the light absorbers.20 Consequently, the brightness is highly decreased, resulting in broad distribution in reflection spectra. It is this feature that frees us from the burden of post-treatments, thus providing an easy way to fabricate low angle-dependent photonic crystals without sacrificing the color brightness.

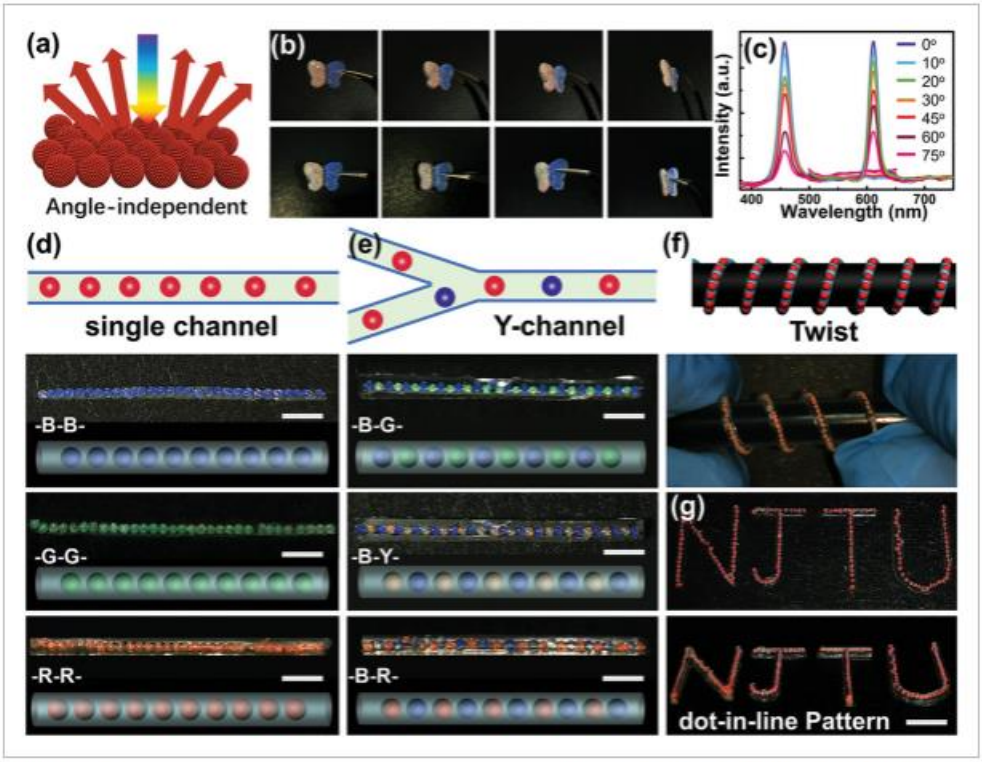

Figure 4 Open in figure viewer | PowerPoint

a) Cartoon illustration of angle-independence of the photonic gel. b) Photographs of a butterfly-shaped photonic gel at different viewing angles. c) Reflectance spectra of the red and blue part of the butterfly-shaped photonic gel at varying detection angles from 0° to 75°. d,e) Microfluidics-assisted assembly of linear photonic gel. Linear photonic gel with (d) one kind of colloidal crystal and (e) two kind of colloidal crystal were prepared by single and Y-type channel. Scale bar is 1 mm. f) 3D spiral photonic hydrogel. g) The optical images of structural color pattern prepared by injectable photonic precursor hydrogel solution. Scale bar is 2 mm.

In addition, by integrating the IPH with the microfluidics-assisted assembly method, we attempted to develop dot-in-line colloidal crystal fibers and structural color-encoded fibers in a controllable fashion. As shown in Figure 4d, a single channel was employed to form the linear colloidal crystal

fiber with homogeneous structural color. Specifically, by pumping the mixture of hydrogel precursor and photonic supraballs into a tapered round glass capillary with diameter around 500 μm at the orifice, the photonic supraballs would line up and assemble into a linear arrangement. The color of the colloidal crystal fibers could be adjusted according to the size of PS@poly(HPA-co-VI). Analogously, a Y-channel with two inlets was engineered to make the structural color-encoded fibers (Figure 4e). As a result, a series of colloidal crystal fibers with two colors arranged alternately were achieved, such as blue-green (-B-G-), blue-yellow (-B-Y-) and blue-red (-B-R-) sequence. Intriguingly, the colloidal crystal fiber could be freely twisted and attached onto a cylinder, showing superior flexibility (Figure 4f). Besides, with the aid of custom-built molds, structural color patterns comprising of close-packed linear photonic supraballs could be fabricated with retention of their angle-independent optical response (Figure 4g). In terms of the easy processing, it is technically possible to prepare colloidal crystal fibers with arbitrary length and we have obtained a colloidal crystal fiber of about 10 cm in length (Figure S7, Supporting Information).

2.4 The Application of IPH in Reflective Cooling

The second set of experiments was focused on investigating the heat-insulating performance of the photonic gel based on its inherent PBG behavior. Currently, passive reflective cooling technique is considered promising to solve the rapidly increasing global warming problem.21 In this respect, heat-insulating films, engineered by Bragg reflectors that selectively reflect light within a specific range of wavelengths is a promising candidate to solve this problem (Figure 5a).22 Infrared photographs of GelMA/CD/poly(HPA-co-VI) hydrogel sample and photonic hydrogel (stopband at 700 nm) irradiated at different time are shown in Figure 5b. After irradiation, the temperature of photonic hydrogel with a stopband of 700 nm increased from 25.1 to 56 °C, while the temperature of GelMA/CD/poly(HPA-co-VI) hydrogel samples increased from 25.0 to 67.8 °C. The temperature of photonic gel was 11.8 °C lower than the blank GelMA/CD/poly(HPA-co-VI) hydrogel sample after exposure to 90 s of sun irradiation, demonstrating ≈48% increase in heat-shielding efficiency. We then investigated the influence of stopband position on thermal insulation. The surface temperature of a structural color film after 90 s of simulated sun irradiation (light intensity of 100 mW cm−2) decreased with the increase of the stopband position (Figure 5c), which is consistent with our previous study. This is because the photonic crystal with higher stop band can reflect more near-infrared radiation. From the perspective of practical application, we presented the outdoor heat-shielding performance of the photonic gel on a sunny day in Nanjing, China, by exposing it to sunlight from 10:00 to 14:00 (Figure S8, Supporting Information). Comparing with the blank hydrogel substrate, maximal temperature differences of 10.2, 11.4, 14.7, and 17.4 °C can be achieved from different reflections (stop band at 456, 551, 625, and 700 nm), respectively (Figure 5d). These results suggested that photonic crystal films are effective in passive solar reflective cooling through their inherent PBG characteristics. In our previous work, the influence of structural colors on thermal insulation was preliminarily studied.23 However, owing to the complexity in real application environment, it is still challenging to predict the outdoor passive reflective cooling performance of photonic crystal films. In this case, we employed the angle-independent photonic gels to the study of outdoor passive reflective cooling and inspiring results were obtained. Our findings present an alternative way to develop cooling materials that take advantages of PBG to suppress solar irradiance during daytime.

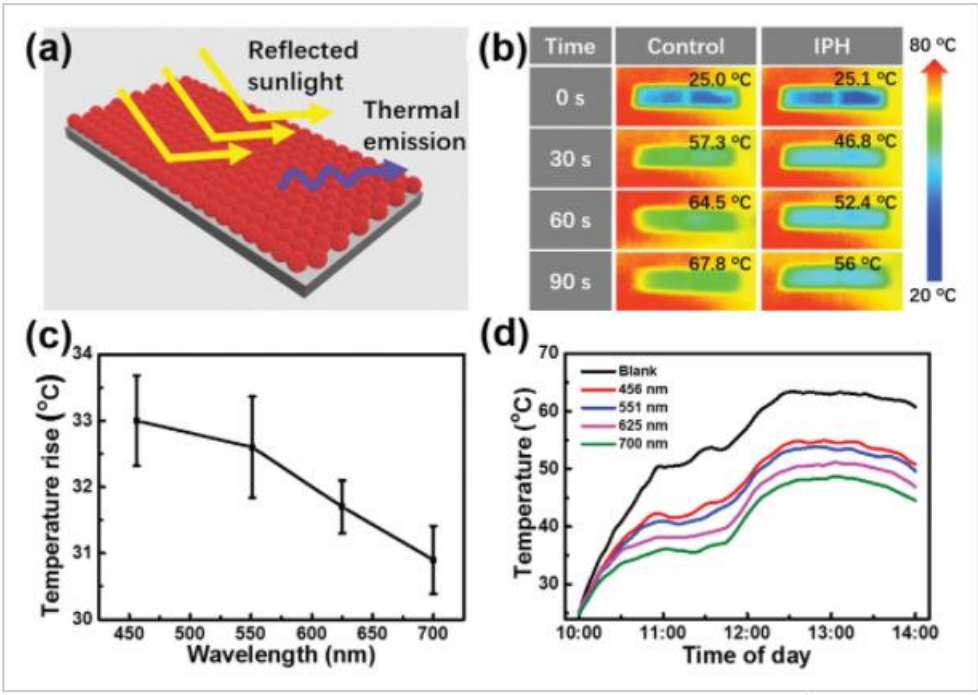

Figure 5

Open in figure viewer | PowerPoint

a) Schematic of mechanism of reflective cooler prepared by photonic hydrogel. b) Infrared photographs of GelMA/CD/poly(HPA-*co*-VI) hydrogel sample and photonic hydrogel (stopband at 700 nm) depending on irradiation time. c) The temperature rises of structural colors versus reflection peaks after 90 s of irradiation. d) The temperature changes for the black paper in the box covered with glass substrate and photonic hydrogel with different reflection peaks depending on time of the day.

3 Conclusion

In summary, we propose an available easy-to-perform strategy for facilely curing colloidal photonic crystals structural colors in a large-scale and fast fashion by combining microfluidics-derived CPC supraballs (structural coloration material) with self-healable hydrogel (scaffold), generating injectable photonic hydrogel in-situ. This new kind of IPH offers both advantages of self-healable (based on hydrogen bonds and host-guest interactions) and temperature-controllable features. Thus, in virtue of a microfluidics-assisted assembly method, a series of linear, planar and spiral assemblies with flexible structures and angle-independent spectrum characteristics can be facilely and fast realized in a large-scale fashion, which might guide and stimulate the development of various macroscopic architectures. In addition, by taking advantage of the inherent photonic bandgap behavior, an application of such photonic gels in reflective cooling was demonstrated, and a maximum value of 17.4 °C in real outdoor solar reflective cooling was attained. This work aims to present a feasible and flexible strategy for the construction of IPH, as well as to provide novel insights into microfluidics-assisted macroscopic self-assembly toward thermal management applications.

4 Experimental Section

Chemicals and Materials: Styrene (St), 2-hydroxypropyl acrylate (HPA), N,N-methylenebisacrylamide (MBAA), and N-vinylimidazole (VI) were purchased from Aladdin Industrial Corporation and were purified by decompressing distillation before usage. 2-hydroxy-4′

-(2-hydroxyethoxy)-2-methylpropiophenone (I2959) was obtained from Sigma-Aldrich. Gelatin, methacrylate anhydride, β-cyclodextrin (CD) and polyvinylpyrrolidone (PVP, K40, Mw = 40 000), were received from Sinopharm Chemical Reagent Co., Ltd.. Methylsilicone oil was purchased from Dow Corning Corporation. Purified water with resistance greater than 18 MΩ cm was used in the experiments. All other chemicals were used as received.

Synthesis of Monodisperse Polystyrene@poly(2-hydroxypropyl acrylate-co-N-vinylimidazole) (PS@poly(HPA-co-VI)) Core/Shell Colloidal Microspheres: Seed emulsion polymerization was carried out to synthesize the core/shell microspheres. Briefly, a homogeneous solution consisting of 0.24 g PVP, 0.3 g NaHCO3, and 110 g deionized water was poured in a 250 mL round flask. The solution was stirred under nitrogen atmosphere and heated to 98 °C, followed by addition of 6.0–10.0 g of St and 0.04 g of KPS dissolved in 12 g deionized water dropwise. The reaction was continued for 1.5 h. Appropriate mounts of HPA, VI, and KPS dissolved in water were then added into the solution and the reaction was continued for another 5 h. The typical composition is VI/HPA = 2:1 mol/mol, and KPS = 0.1 wt%.

Fabrication of the Photonic Supraballs: A single-emulsion glass capillary microfluidics, was used to prepare the photonic supraballs, consisting two syringe pumps and a microfluidics chip. The microfluidics chip was assembled based on a previously published procedure. Two round capillaries were tapered by a pipette puller (Sutter Instrument, Inc.) and sanded to 50 and 100 μm in diameter, respectively. Then, the two round capillaries were aligned in a square capillary. Finally, these tubes were fixed and sealed by an epoxy resin. The inner phase (10–50 wt% PS@poly(HPA-co-VI) latex) and outer phase (Methylsilicone oil with 5 wt% surfactant) were pumped into the capillary microfluidics device by syringe pumps (Nanjing Janus New Materials Co., Ltd). Typical flow rates for the inner and outer phases were 0.1 and 10 mL h−1, respectively. Then, the microdroplets were collected into a spawn bottle. The obtained microdroplets were dried in ambient condition overnight.

Synthesis of GelMA: Briefly, 8.0 mL of methacrylic anhydride was added dropwise into type A porcine skin gelatin solution (10.0 g in 100 mL Dulbecco's phosphate-buffered saline, DPBS) for reaction for 3 h at 50 °C. Afterward, 1 week dialysis with 12–14 kDa cut-off was performed to remove salts and unreacted methacrylic anhydride, followed by 1 week lyophilization. The resultant white porous foam was stored at −80 °C until further use.24

Preparation of Photonic Gels: First, the hydrogel precursor was prepared by simply dispersing appropriate mounts of HPA, VI, MBA, and I2959 dissolved in GelMA solution (1 g of GelMA dissolving in 5 g of DI water). The typical composition is VI/HPA = 2:1 mol/mol, MBAA = 0.1 wt%, and I2959 = 0.1 wt%. Then, a proper amount of photonic supraballs were homogenously dispersed in the hydrogel precursor and added into a syringe. After injecting the mixture into a specially prepared mold, it was polymerized to form a hydrogel by exposing to UV light for 60 s. Finally, the photonic gel was peeled off from the mold.

Self-Healing of Photonic Hydrogels: The healing process was finished by mechanically brought two halves into contact. The two parts of sample were stuck together and were pressed for more than 1 min. After several minutes, the joint fused and the photonic hydrogels self-healed at ambient

temperature.

Characterization: Nicolet 6700 FT-IR spectrometer was utilized to collect Fourier-transform infrared spectra. Thermo Scientific Nicolet iN10 infrared microscope equipped with a liquid nitrogen cooled MCT detector (Thermo Electron Corporation, USA) was used to collect Micro-IR images. Scanning electron microscopy using a HITACHI S-4800 scanning electron microscope was utilized to observe the morphologies of materials. An optical microscope equipped with a fiber optic spectrometer (Ocean Optics, USB4000) was used to record the reflection spectra. Dynamic light scattering (DLS) (Malvern, ZEN3690) was used to measure the size and zeta potential of materials. Fluke Ti30 IR thermal imager was utilized to record the temperature profiles. SHUNYU SZM45 stereoscopic optical microscope with color CCD camera was used to take the optical images. The mechanical tensile stress versus strain was tested by a SANS CMT6203 testing machine at ambient temperature. A stress-controlled rheometer (Anton paar MCR302) was utilized to take rheological characterization. The viscosity of hydrogel precursor as a function of the temperature (5.5–50 °C) was measured using rotational viscometry with a cone and plate geometry (plate diameter 50 mm, distance 0.108 mm at 5 rad s−1).

Acknowledgements
Z.Z. and J.-D.L. contributed equally to this work. This work was supported by National Natural Science Foundation of China (21736006), National Key Research and Development Program of China (2016YFB0401700), Fund of State Key Laboratory of Material-Oriented Chemical Engineering (ZK201704, KL18-05), Start-Up Fund (1-ZE7S) and Central Research Fund (G-YBWS) from the Hong Kong Polytechnic University.

Conflict of Interest
The authors declare no conflict of interest.\

[1] G. Liu, M. Cai, F. Zhou, W. Liu, J. Phys. Chem. B 2014, 118, 4920.
[2] T. Sun, Y. L. Sun, H. Y. Zhang, Polymers 2018, 10, 513.
[3] S. N. Jha, R. P. Kachru, J. Food Process Eng. 1998, 21, 301.
[4] M. Shankar, N. Chaudhary, D. Singh, Int. J. Pharm. Biol. Arch. 2010, 1, 101.
[5] Q. Zhang, F. Liu, K. T. Nguyen, X. Ma, X. Wang, B. Xing, Y. Zhao, Adv. Funct. Mater. 2012, 22, 5144. [
6] L. He, Y. Huang, H. Zhu, G. Pang, W. Zheng, Y. S. Wong, T. Chen, Adv. Funct. Mater. 2014, 24, 2754.
[7] C. de la Torre, I. Casanova, G. Acosta, C. Coll, M. J. Moreno, F. Albericio, E. Aznar, R. Mangues, M. Royo, F. Sancenón, R. Martínez-Máñez, Adv. Funct. Mater. 2015, 25, 687.
[8] L. Palanikumar, E. S. Choi, J. Y. Cheon, S. H. Joo, J. H. Ryu, Adv. Funct. Mater. 2015, 25, 957.
[9] W. Ngamcherdtrakul, J. Morry, S. Gu, D. J. Castro, S. M. Goodyear, T. Sangvanich, M. M. Reda, R. Lee, S. A. Mihelic, B. L. Beckman, Z. Hu, J. W. Gray, W. Yantasee, Adv. Funct. Mater. 2015, 25, 2646.
[10] Z. Li, J. Barnes, A. Bosoy, J. F. Stoddart, J. Zink, Chem. Soc. Rev. 2012, 41, 2590.
[11] Y. L. Sun, H. Y. Zhang, Y. X. Wang, Y. Wang, J. Controlled Release 2017, 259, e45.
[12] Y. Sun, Y. Yang, J. Controlled Release 2013, 8, 181.

[13] Z. Qu, H. Xu, H. Gu, ACS Appl. Mater. Interfaces 2015, 7, 14537.
[14] T. Ribeiro, E. Coutinho, A. S. Rodrigues, C. Baleizão, J. P. S. Farinha, Nanoscale 2017, 9, 13485.
[15] D. R. Radu, C. Y. Lai, J. W. Wiench, M. Pruski, V. S. Lin, J. Am. Chem. Soc. 2004, 126, 1640.
[16] C. Boyer, N. A. Corrigan, K. Jung, D. Nguyen, T. K. Nguyen, N. M. Adnan, S. Oliver, S. Shanmugam, J. Yeow, Chem. Rev. 2016, 116, 1803.
[17] J. Klein, Science 2009, 323, 47.
[18] S. Jahn, J. Seror, J. Klein, Annu. Rev. Biomed. Eng. 2016, 18, 235.
[19] J. Klein, Friction 2013, 1, 1.
[20] J. Seror, L. Zhu, R. Goldberg, A. J. Day, J. Klein, Nat. Commun. 2015, 6, 6497.
[21] M. Kobayashi, A. Takahara, Chem. Rec. 2010, 10, 208.
[22] J. Seror, Y. Merkher, N. Kampf, L. Collinson, A. J. Day, A. Maroudas, J. Klein, Biomacromolecules 2011, 12, 3432.
[23] G. Liu, Z. Liu, N. Li, X. Wang, F. Zhou, W. Liu, ACS Appl. Mater. Interfaces 2014, 6, 20452.
[24] M. Kobayashi, M. Terada, A. Takahara, Faraday Discuss. 2012, 156, 403.
[25] X. Zhu, C. Yan, F. M. Winnik, D. Leckband, Langmuir 2007, 23, 162.
[26] J. Israelachvili, Intermolecular and surface forces, 2nd ed., Academic Press, San Diego, CA 1991.
[27] H. Iijima, T. Aoyama, A. Ito, J. Tajino, M. Nagai, X. Zhang, S. Yamaguchi, H. Akiyama, H. Kuroki, Osteoarthritis Cartilage 2014, 22, 1036.
[28] Y. Sun, B. Yang, S. X. Zhang, Y. Yang, Chem. - Eur. J. 2012, 18, 9212.
[29] Y. Sun, Y. Yang, D. Chen, G. Wang, Y. Zhou, C. Wang, J. F. Stoddart, Small 2013, 9, 3224.
[30] H. Y. Zhang, Y. F. Sun, Y. L. Sun, M. Zhou, Bio-Med. Mater. Eng. 2014, 24, 2211.
[31] Y. Wang, W. G. Cui, X. Zhao, S. Z. Wen, Y. L. Sun, J. M. Han, H. Y. Zhang, Nanoscale 2018, https://doi.org/10.1039/C8NR07329E.
[32] F. Sun, Y. Li, N. Zhang, J. Nie, Polymer 2014, 55, 3656.
[33] H. Y. Zhang, J. B. Luo, M. Zhou, Y. Zhang, Y. L. Huang, J. Mech. Behav. Biomed. Mater. 2013, 20, 209.
[34] H. Y. Zhang, S. H. Zhang, J. B. Luo, Y. H. Liu, S. H. Qian, F. H. Liang, Y. L. Huang, J. Tribol. 2013, 135, 032301.
[35] H. Y. Zhang, Y. J. Zhu, X. Y. Hu, Y. F. Sun, Y. L. Sun, J. M. Han, Y. Yan, M. Zhou, Bio-Med. Mater. Eng. 2014, 24, 2151.
[36] Y. Y. Jiao, S. Z. Liu, Y. L. Sun, W. Yue, H. Y. Zhang, Langmuir 2018, 34, 12436.
[37] A. Mirando, Y. Dong, J. Kim, Methods Mol. Biol. 2014, 1130, 267.
[38] C. Li, K. Chen, H. Kang, Cell Death Dis. 2017, 8, e3165.
[39] K. P. H. Pritzker, S. Gay, S. A. Jimenez, K. Ostergaard, J. P. Pelletier, P. A. Revell, D. Salter, W. B. van den Berg, Osteoarthritis Cartilage 2006, 14, 13